Journal of Applied Polymer Science

Effect of Borax Addition on the Structural Modification of Bentonite in Biodegradable Alginate-Based Biocomposites

Birgül Benli
Mineral Processing Engineering Department, Istanbul Technical University, Maslak 34469, Turkey
Correspondence to: Dr. B. Benli (E-mail: benli@itu.edu.tr)

ABSTRACT: Functionalized next generation biodegradable polymeric systems (bioplastics) that have better compatibility, enhanced relaxation, and thermal properties were designed using bentonite-added alginate biocomposite films in the presence of borax. A series of bentonite-added biocomposite films crosslinked with $CaCl_2$ were characterized by using methods like XRD, FTIR, TGA, DTA/DSC, DMA, and AFM. A plausible structural mechanism with Ca^{2+} crosslinking gel formation known as egg-box and borate ion complexes was proposed to elucidate the interactions between borax and bentonite/alginate biocomposites. Enhanced compatibility and hybrid properties of raw fillers were confirmed by mineral processing steps involving hydrocyclone purification for bentonite and recrystallization steps for borax. The structure of bentonite and also bentonite hybrid biocomposites were clearly improved upon small additions of borax into the matrix. The presence of borax was found to provide a more intercalated or exfoliated morphology for a given hybrid biocomposite structure. Borate ions dissociated in aqueous solution provided a better effect on the intercalation of bentonite by imparting new hydrogen bonding sites, diol-complexes, and didiol-crosslinking gels. © 2012 Wiley Periodicals, Inc. J. Appl. Polym. Sci. 128: 4172–4180, 2013

KEYWORDS: self-assembly; polysaccharides; clay; properties and characterization; gels

Received 16 July 2012; accepted 19 September 2012; published online 18 October 2012
DOI: 10.1002/app.38609

INTRODUCTION

Biodegradable alginate composites are becoming increasingly attractive for short-term application materials, e.g., edible films, coatings, and packaging materials in areas other than biomedical applications. These applications also include biocomposites as an alternative to petroleum-based polymers "traditional plastics".[1,2] Development of the green, sustainable, recyclable, and biodegradable plastics gives new approaches to solving the ecological problem for the disposal of plastic wastes.[3] Remarkable products that offer commercial biodegradable bioplastics are prepared from chemically modified natural sources; e.g., cellulose, lignin, protein,[4] chitin-chitosan[5], and especially, starch.[2,6,7] However, these natural polymers do not always possess the characteristics desired in plastics. In recent years, new generation bioplastics called nano-biocomposites has been formulated and associated with nano-sized fillers (Alexandre and Dubois, 2000; Bordes et al., 2009).[8,9] For biodegradable polymers, typical examples of inorganic fillers are based on industrial minerals and mainly clays including carbon black, graphite, carbon nanotubes, talc, mica, ultra-fine layered titanate,[10] hydroxyapatite,[4] and sepiolite[6] as well as rectorite, hectorite, saponite, and montmorillonite among smectite-type layered silicates.[11–13]

Alginate is a well-known anionic polysaccharide distributed widely in the cell walls of brown algae. The structure of alginate (Figure 1) is mainly a family of unbranched binary copolymer with homopolymeric blocks consisting of (1-4)-linked β-D-mannuronate (M), and its C-5 epimer α-L-guluronate (G) residues, respectively.[14,15] Alginate has a unique property in that it forms an insoluble gel, known as egg-box junction in the presence of multivalent cations[16] like Ca^{2+}. Alginate bound with monovalent ions is generally water soluble whereas covalently crosslinked together with divalent ions forms hydrogels of partially soluble in water.[16,17]

New trends in the last decade combined the fillers or functionalized minerals in order to improve the performances of bioplastics,[18–20] suggested that anion type of gelling agents such as borate, titanate, or antimonite[21] are very useful to increase the compatibility between filler and polymer matrix. The presence of second filler not only prevents the formation of the clay aggregate but also aids the formation of exfoliation of clay platelets in the polymer matrix. Among them, borax ($Na_2B_4O_7.10H_2O$ or sodium tetraborate) has been used as crosslinking agents for water-soluble polymers such as partially hydrolyzed polysaccharides or polyacrylamides.[21,22] The basic structure of borax contains chains of interlocking $BO_2(OH)$

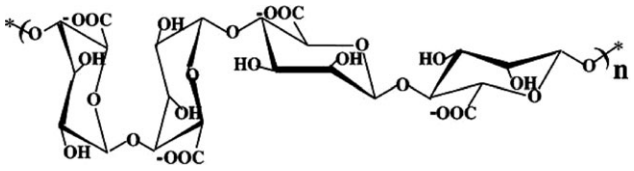

Figure 1. Chemical structure of alginate.

triangles and $BO_3(OH)$ tetrahedrons bonded to chains of sodium and water octahedrons. From monodiol and didiol complexation reactions,[21,22] well-known complexes form between borate and simple polyols of alginate due to the fact that there are numerous hydroxyl groups on sodium alginate chains. Although the preparation and characterization of alginate biocomposites have been extensively studied using several fillers such as Ca-bentonite,[23] hydroxyapatite,[14,24] rectorite,[11] layered double hydrates,[12] and silica,[25] the effect of borax addition as a second filler into biopolymer and filler composite systems has not been studied.

The aim of this study is to investigate the effect of borax addition on the alginate/bentonite biocomposite films. First, the raw fillers, i.e., bentonite and borax were prepared to enhance the compatibility of alginate biopolymer matrix and also improve filler-matrix adhesion by purification and recrystallization steps, respectively. Second, the morphological and chemical properties of filler/alginate biocomposites were characterized by XRD, FTIR, thermogravimetric analysis (TGA), differential scanning calorimeter (DSC), dynamic mechanical analysis (DMA), and Atomic Force Microscopy (AFM) in order to identify the interaction mechanisms between borax and alginate/bentonite biocomposites.

EXPERIMENTAL

Materials

Natural sodium bentonite sample was obtained from Resadiye (Tokat, Turkey). The raw bentonite sample was dispersed in tap water at room temperature for 48 h and then subjected to a multistage purification process using multi-hydrocyclone separator.[26,27] The sample was dried and gently ground for further use. Under the optimum conditions, high purity concentrate with cation exchange capacity of 98 meq/100 g based on a standard method of methylene blue test and average particle size of 2.5 μm with Fristch Laser Particle Sizer was obtained. The chemical compositions of the samples were accomplished with Inductively Coupled Plasma Spectrometer (ICP) in ACME Analytical Lab., Canada. The chemical composition (wt %) of the purified bentonite (Na-montmorillonite) is given as SiO_2 60.11; Al_2O_3 17.90; TiO_2 0.31; Fe_2O_3 3.66; MnO 0.02; MgO 2.33; CaO 0.75; K_2O 0.31; Na_2O 2.54; P_2O5 0.04; and ignition loss 12.00.

Borax (sodium tetraborate decahydrate) was crystallized from industrial grade borax pentahydrate of Etimaden of Turkey. A saturated solution of borax pentahydrate was prepared according to the solubility data of Mullin.[28] Borax pentahydrate was dissolved in a crystallizer for purification and production of the borax decahydrate. The solution was then heated above the saturation temperature (~69°C), and the required quantity of Na_2CO_3 was added to the solution in order to precipitate probertite. The precipitated probertite was removed from the hot solution using a filter press. Finally, the purified hot solution was cooled to room temperature. The crystals obtained were dried at room temperature. In the second step of borax purification, the crystals were purified by recrystallization without adding Na_2CO_3. Borax completely dissociates into borate ions ($B_4O_7^{2-}$), and boric acid in aqueous solutions and an acid-base equilibrium between boric acid and monoborate ions.[21,22] Sodium alginate was purchased from Sigma-Aldrich as alginic acid of sodium salt from brown algae. Its grade is specifically recommended for immobilization applications.

Preparation of Filler Added Alginate Biocomposite Films

Biocomposite films were prepared by casting and solvent evaporation technique at room temperature. The desired quantity of sodium alginate was hydrated overnight in deionized water (18 MΩ.cm, obtained using a Milli-Q System, Millipore) to facilitate the dissolution of alginate and to obtain alginate solutions of 1 and 3 wt %. The appropriate amount of filler material into the biopolymer solution was added on a magnetic stirrer at 100 rpm. Then, the dissolved composite solutions were cast onto clean glass plates of 10 × 20 cm in size with the aid of a casting knife at room temperature. Then, all the samples were soaked in a bath of 20 wt % $CaCl_2$ solution for half an hour. After producing cross-linked films, the films were taken out of the reaction solution, rinsed twice with ethyl alcohol to strengthen the film, and then washed with demineralized water to eliminate any possible residues and remaining traces of solvent. After drying the films for 3 days in a box, thicknesses of dried films ranging from 45 to 50 μm were obtained.

Characterization of Filler Added Alginate Biocomposite Films

XRD measurements of biocomposite films were performed using a Rigaku, Miniflex model X-ray diffractometer equipped with Cu-Kα radiation at room temperature; this is to identify the smectite groups and other associated impurities and crystalline phases of native organic polymer. The samples were scanned up to 60° in 2θ (where θ is the Bragg angle) in a continuous mode.

The IR spectra for pure alginate films and filler (bentonite and borax)-added alginate biocomposites were conducted with Perkin Elmer brand FT-IR Spectrometer to identify the biocomposite structure and to determine the presence of any free COO^- or any other bonds in the polymer matrix.

Thermal stabilities of the biocomposite films were examined with Perkin Elmer TG/DTA Analyzer in the temperature range of 50–530°C at a heating rate of 20°C/min under nitrogen atmosphere. Also, DSC was used on a DSC Q10 V8.1 adjusted to a heating rate of 10°C/min. The samples were subjected to DSC measurements before and after adding fillers to determine their thermal stability and decomposition characteristics.

The dynamic mechanical properties of the alginate and filler added alginate composite films were carried out with a Dynamic Mechanical Thermal Analyzer DMA V (Rheometric Scientific, Leatherhead, UK) at 1 Hz and heating rate of 2°C/min, in order to characterize the dynamic mechanical spectra, mechanical damping δ, storage modulus E', and loss modulus E''. In these measurements, all composite films were cut into rectangular strips of approximately 0.1 × 10 × 40 mm in dimension.

Applied Polymer SCIENCE

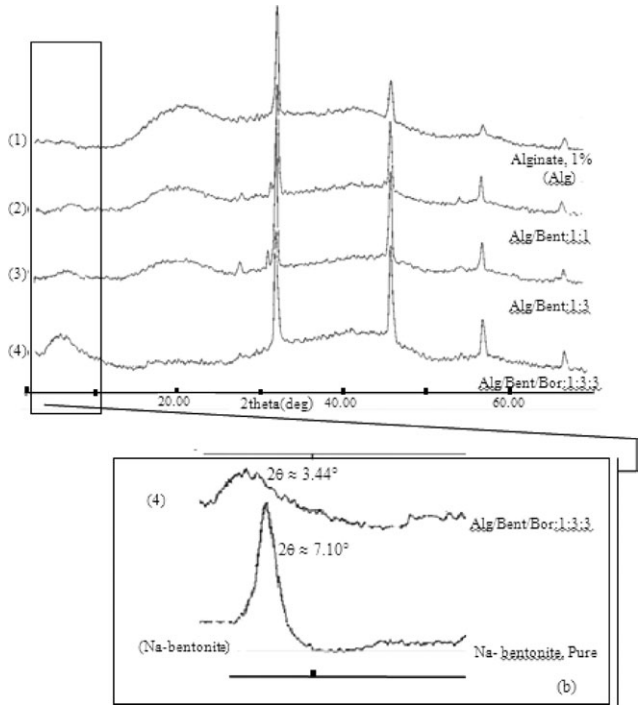

Figure 2. XRD patterns of pure alginate 1 wt % (1), its biocomposites with different bentonite ratios as 1 : 1 (2) and 1 : 3 (3), borax-modified bentonite-alginate biocomposite in the ratio of 1 : 3 : 3 for alginate, bentonite, and borax, respectively (4).

AFM (Park System, XE 70) was used to examine the surface topography of the alginate-based biocomposite films. The AFM measurements were performed with moisture controlled ambient conditions (22 ± 2°C) in the noncontact mode using 910 M-NSC14/Cr–Au-type cantilevers with 0.5 Hz scanning speed. Cantilevers were exposed to UV/O_3 (UV Cleaner, Bioforce Nanosciences) for 15 min before each experiment to remove any possible contamination on each probe. Section analysis, roughness, and power spectral density measurements were calculated using XEI image analysis software from Park System.

RESULTS AND DISCUSSION

The importance of borax as a second inorganic filler in the bentonite-added alginate biocomposite films has been studied in order to achieve new generation of functionalized biopolymer composites.

XRD Analyses

The XRD patterns of Ca-crosslinked films (Figures 2 and 3) in two different biopolymer concentrations (1 and 3 wt % of alginate) revealed that the structures of hybrid biocomposite films were definitely improved upon borax addition into the system.

Pure alginate films show significant five crystalline peaks: the first one being at about between 15° and 23° and other diffraction peaks which correspond to the crystalline phases of alginate occur around 31.6°, 45°, 56°, and 65° (Figures 2 and 3). Also, sharper diffraction peaks indicate the existence of cross-linking mechanism taking place in some large junction zones described in the literature as "egg-box model."[29] In our case, it is clear that egg-box model was also dominant mechanism for molecular interactions between filler and alginate. Additional mechanisms were also noted depending on the filler content and borax addition. In Figure 3, when the ratio of bentonite was kept low (alginate to bentonite ratio of 1 : 1), the biocomposite film showed a peak at 5.32° (1.65 nm), increasing the bentonite ratio to 1 : 3 in the film, the characteristic pattern decreased to 4.84° (1.81 nm) as a result of the intercalation of bentonite layers. Similar results on filler content and intercalation structure were also observed by Benli et al.[30] Suggestions for possible structural models between Ca-bentonite and Na-alginate gels mostly depend on variation in the filler content. When lower filler bentonite contents are dispersed in alginate solution, the filler particles exhibit exfoliated or disordered state whereas increasing the amount of filler to moderate and higher solids contents, leads to intercalated and encapsulated states, respectively.[8] However, the addition of small amounts of borax plays an interesting role for given hybrid biocomposite structure as borate ions dissociated in aqueous solution provide a synergistic effect.[21] The characteristic peak of bentonite at about 2θ ≈ 7.10° (1.24 nm) shifted to the peak 2θ ≈ 3.44° (2.55 nm) as a result of borax addition to the alginate biocomposites.

However, a broad diffraction peak that corresponds to the fast gelatinization Ca-alginates in a metastable form was ascribed to defective crystals and a low crystallinity of alginate.[29] Figure 3 shows that this broad diffraction peak at 2θ of 7.10° was found to relatively decrease after the addition of bentonite filler. The trend of decrease in the 2θ peak continued with increasing the bentonite concentration and borax (second filler) addition in alginate biopolymer, respectively.

XRD patterns of borax and bentonite-added alginate biocomposites in view of egg-box model have not exhibited the characteristic peaks for bentonite at about 2θ ≈ 7.10° observed in denser alginate using divalent cation crosslinker. However, remarkable improvements have been achieved in the borax-added dispersions and/or intercalation of fillers added films due to the increased hydrogen bonding,[31] increased spreading and networking of

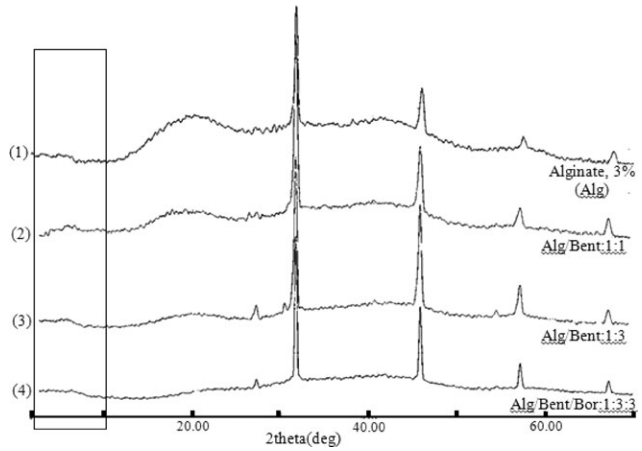

Figure 3. XRD patterns of pure alginate 3 wt % (1), its biocomposites with different bentonite ratios as 1 : 1 (2) and 1 : 3 (3), borax-modified bentonite-alginate biocomposite in the ratio of 1 : 3 : 3 for alginate, bentonite, and borax, respectively (4).

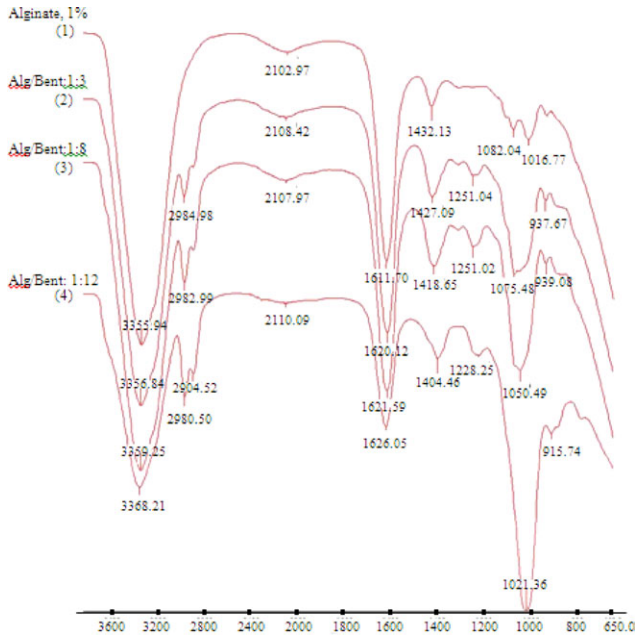

Figure 4. FTIR spectra of the pure alginate (1 wt %) film (1), and three composite films of different alginate-bentonite ratios. [Color figure can be viewed in the online issue, which is available at wileyonlinelibrary.com.]

borate ion-added-crosslinks between alginate chains,[20] and together with the complexation of borate ions and sugar units of alginate.[21] Similarly, rapid gelation observed in the presence of small amounts of borax is attributed to the slightly alkaline pH of the medium as well as the ability of borax to complex with hydroxyl groups of polysaccharides[32]; this means that intermolecular hydrogen bonds between alginate, bentonite, and borax destroyed the original molecular structure of alginate, leading to changes in diffraction patterns similarly to these polymeric blend films between alginate and polyacrylamide.[33] Another possibility of spontaneous polymer spreading over the filler surface which is a basic condition for the design of polymer-mineral composites[34] can be seen after increasing the alginate biopolymer concentration up to three-fold (Figure 3).

The compatibility of bentonite and borax with alginate was detailed in our previous studies by AFM performed Direct Force Measurements using prepared Colloidal Alginate Probe.[23] In the same study, when the bulk concentration of alginate film surface was increased three-fold, adhesion forces of alginate probe and surfaces also changed nearly three-fold. As a result of more compacted structure of alginate surfaces, the adhesion forces calculated from our previous AFM adhesion force measurements are as follows:[23]

3 wt % alginate > Borax > Na-Bentonite > 1 wt % alginate

Although hydrophilic characteristics of alginate biopolymers are more compatible with borax than bentonite, the comparison of alginate-alginate interactions with the fillers depends on the concentration of biopolymer concentration. The magnitude of above adhesion forces, this change complies with the XRD patterns of filler added alginate biocomposite films. Especially, it is important to recognize that as 3 wt % of alginate has the lowest free energy of adhesion, higher concentration of biopolymer improves the dispersion of fillers into the biopolymer and exhibits exfoliated structure but may also offer the evidence of disordered intercalation (Figure 3).

FTIR Analyses

FTIR analyses provide important evidences to interpret the bonding in composite structures. The width and intensity of spectral bands, as well as the position of the peaks are all sensitive to the intermolecular interactions on the molecular level.[33] In this context, intermolecular interactions occur if polymer and filler are compatible, though the spectral information also helps to control their affinity during preparation of high-quality filler added biocomposites. Figure 4 shows the FTIR spectra of pure alginate and three of different biopolymer-clay ratios in the range of 4000–650 cm^{-1}. Table I also lists the functional groups available in the literature on the filler added alginate biocomposite.[35,36]

Figure 4 demonstrates that increasing the amount of bentonite enhances the molecular interactions between alginate and filler, i.e., compatible filler effect. The characteristic band of alginate at 3355 cm^{-1}, that of hydroxyl groups, the asymmetric —COOH stretching vibration and symmetric —COOH stretching vibration was observed at 1625 and 1432 cm^{-1}. The OH stretching peak at 3355 cm^{-1} becomes a little narrower and shifted to 3356, 3359, and 3368 at higher bentonite ratios.

Table I. Assignments of FTIR Absorption Bands for Bentonite-Added Sodium Alginate Biocomposites

Wavenumber (cm^{-1})	Assignment
3622	Al—O—H stretching
3360-3440	O—H stretching, hydration
2750	C—H stretching
1608-1611	COO— stretching
	(asymmetric)
1413-1414	COO— stretching
	(asymmetric)
1124-1126	C—C stretching
	C—O stretching
1087-1088	C—O stretching
	C—O—C stretching
1059	O—H bending
1033	Si—O—Si, Si—O stretching
947-950	C—O stretching
	C—H stretching
915	Al—Al—O—H bending
875	Al—Fe—O—H bending
836	Al—Mg—O—H bending
798	Platy form of tridymite
790	Si—O—Al stretchingAl—Mg—O—H stretching
692	Quartz
529	Si—O bending

Applied Polymer SCIENCE

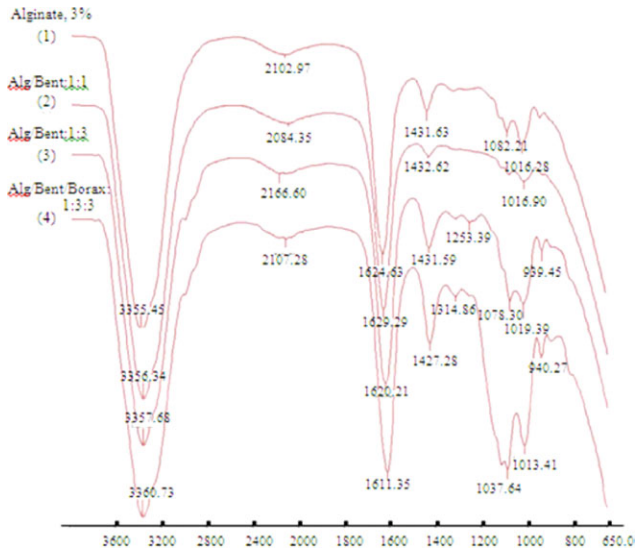

Figure 5. FTIR spectra of the pure alginate film (3 wt %) (1), bentonite-added alginate biocomposite film in the alginate-bentonite ratio of 1 : 1 (2) and 1 : 3 (3), borax-modified bentonite-alginate biocomposite in the ratio of 1 : 3 : 3 for alginate, bentonite, and borax, respectively (4). [Color figure can be viewed in the online issue, which is available at wileyonlinelibrary.com.]

However, the characteristic band of clay at 3622, 1033, 914, and 790 cm^{-1} for the Al—O—H stretching, Si—O—Si, Si—O stretching, Al—Al—O—H, Si—O stretching, Si—O—Al stretching, (Al, Mg)—O—H, and Si—O—(Mg, Al) stretching were not observed at lower bentonite ratios. However, at higher bentonite ratios, shifting and broadening of the Si—O stretching peak at 1021 cm^{-1} together with the structural Al—Al—OH vibration at 915 cm^{-1} confirmed the presence of bentonite in the dispersions.[37] The peak at 1611 cm^{-1} shifting to 1621 and 1626 cm^{-1} suggests the formation of new hydrogen bonds between alginate and bentonite. This can be attributed to the electrostatic interaction between such groups and the negatively charged sites in the clay structure.[38] Furthermore, the peak at 1432 cm^{-1}, which is related to the stretching vibration of carboxylate groups shifted to a lower frequency (1404 cm^{-1}) in the corresponding nanocomposites spectra.[12] This peak is also specific to ionic binding resulting from the calcium ions replacement with sodium ions in the alginate blocks.[35] Another possibility refers to the peaks in the region between 1150 and 1000 cm^{-1}, which have been assigned to C—C and C—O bonds; the interaction of the cross-linker solution with the oxygen sites of alginate and the calcium ions of bentonite, namely, Ca-crosslinking of alginate provides the evidence of encapsulation of bentonite.[14] The effect of borax filler was in bentonite-added alginate biocomposites analyzed by FTIR analysis (Figure 5). Compared to pure alginate and borax-added alginate biocomposite, the detectable changes found at 2800–3000 cm^{-1} may be ascribed to a change in the amount of C—H groups. The peak at 1431 cm^{-1}, which is related to the stretching vibration of carboxylate groups remained the same in bentonite-added composites. However, after borax addition, synergistic effect of borax, the relevant peak shifted to a lower frequency (1427 cm^{-1}) as an evidence of nanocomposite formation.

The intensity of the absorption peak for the C—O—C bond[5] at 1253 cm^{-1}, which is attributed to the chemical bonding between —COO in alginate and —OH was reduced after borax addition as an evidence of diol and polyol units of alginate and borate ion complexes (Figure 6). However, the spectrum of the double filler containing biocomposite films shows a significant difference in the region of the C—O—C asymmetric stretch at around 1100 cm^{-1}. Acidic character of borax led to O—H asymmetric vibrations and induced new hydrogen bonding sites by the addition of bentonite to the alginate biocomposite (Figure 6). Based on the change in the C—O—C band in the spectrum, hydrogen bonding mechanism was suggested for the intercalation of bentonite.[39] These results also confirmed by their XRD patterns provided a synergistic effect of borax addition. The above comments together with XRD and FTIR analyses illustrated the gelling mechanisms of alginate, bentonite biocomposite systems and the effect of borate ion effects on this system can be explained with two possible model structures (Figure 6), and corresponding reactions between borate ions and hydroxyl groups of alginate sugar units lead to monodiol-borate complex formation and between two diol units of alginate chains and one borate ion to the cross-linking formation as didiol-borate complexes.[21]

TGA

Typical weight loss curve of pure alginate and Na-bentonite/alginate biocomposites are shown (Figure 7), and then, the effect of borax addition (5) was also compared with the pure alginate (1), and bentonite/alginate biocomposite in the same graph. TGA curves show a weight loss change at around 100°C. This change from 35% for alginate to 15% for bentonite-added composites was attributed to the loss of physically adsorbed water molecules. The temperature of 10% weight loss of pure alginate (1), bentonite-added alginate biocomposites in ratios of 1 : 3 (2), 1 : 8 (3), and 1 : 12 (4) corresponds to 72, 76, 90, and 110°C, respectively. This increase in thermal stability can be attributed to the high thermal stability of clays and the dispersion of clay particles within alginate.[40] Additionally, the temperatures of 25% weight loss of the above films coincide with 102, 120, 128, and 420°C, respectively. The results clearly show that the decomposition temperature of the bentonite-added alginate biocomposites are higher than that of pure alginate, meanwhile, similar results were found for alginate/Na-rectorite films,[11] chitosan-sepiolite,[38] and alginate-hydroxyapatite.[14]

However, the influence of borax addition to the bentonite/alginate biocomposites was observed especially in the temperatures of 40% weight loss as 190°C (5); this compares to the 160°C of bentonite-added biocomposite film (2), and 140°C of pure alginate film (1). Thermal stability investigations were also continued with 3 wt % pure alginate as three-fold increase of the initial polymer concentration. However, bentonite and borax did not cause a significant increase in the thermal stability of the higher compacted alginate (3 wt %) biocomposites.

Figure 8 shows the DTA/DSC curves for biocomposite films of pure 1% wt of alginate (1), its biocomposites with different bentonite ratios as 1 : 1 (2), 1 : 3 (3), and 1 : 12 (4), borax-modified bentonite-alginate biocomposite in the ratio of 1 : 3 : 3 for

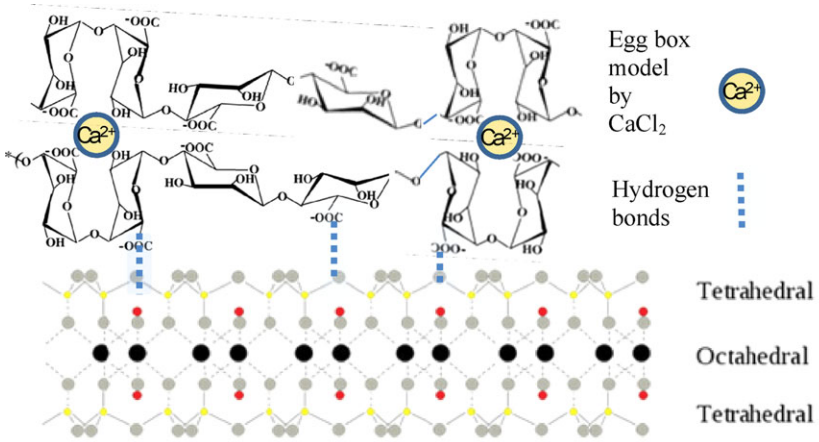

(a) Egg box model by $CaCl_2$ for the bentonite added alginate biocomposite in the absence of borax

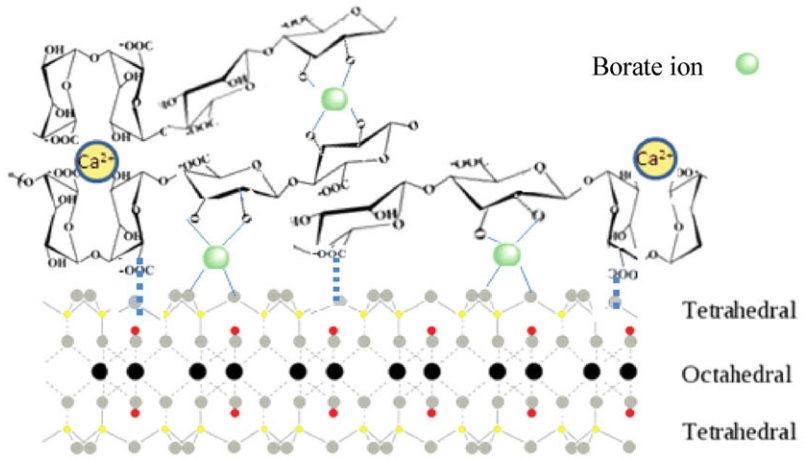

(b) Borate complexes and egg-box model in the presence of borax.

Figure 6. Possible gelling mechanisms of alginate/bentonite biocomposites in the absence (a) and presence (b) of borax. [Color figure can be viewed in the online issue, which is available at wileyonlinelibrary.com.]

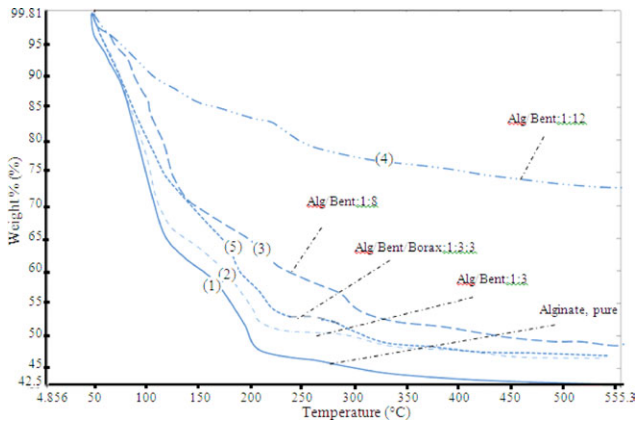

Figure 7. The TGA curves of the pure 1 wt % of pure alginate (1), bentonite-added biocomposite films in ratios of 1 : 3 (2), 1 : 8 (3), 1 : 12 (4), and borax-modified bentonite-alginate biocomposite in the ratio of 1 : 3 : 3 (5) for alginate, bentonite, and borax, respectively. [Color figure can be viewed in the online issue, which is available at wileyonlinelibrary.com.]

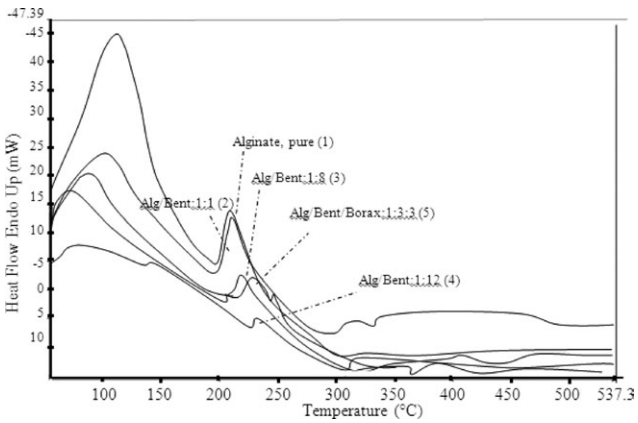

Figure 8. The DTA/DSC curves of the pure 1% wt of pure alginate (1), bentonite-added alginate biocomposite films in ratios of 1 : 1 (2), 1 : 8 (3), 1 : 12 (4), and borax-modified bentonite-alginate biocomposite in the ratio of 1 : 3 : 3 (5) for alginate, bentonite, and borax, respectively.

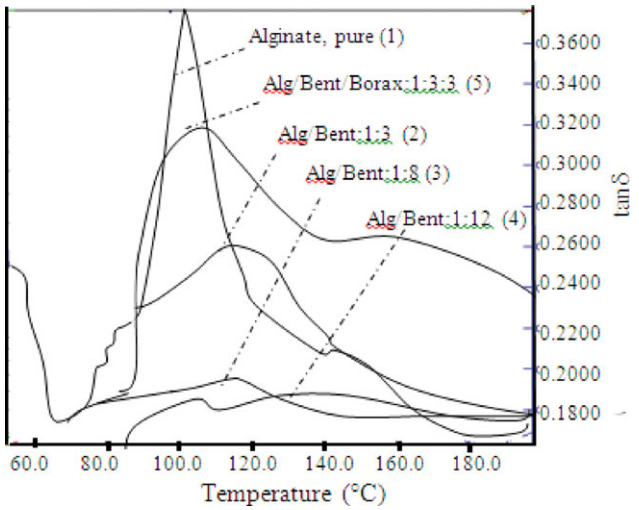

Figure 9. The DMA curves of the pure 1% wt of NaAlg (1), NaBent/NaAlg biocomposite films in ratios of 1 : 3 (2), 1 : 8 (3), 1 : 12 (4), and borax-modified bentonite-alginate biocomposite in the ratio of 1 : 3 : 3 (5) for alginate, bentonite, and borax, respectively. [Color figure can be viewed in the online issue, which is available at wileyonlinelibrary.com.]

alginate, bentonite, and borax, respectively (5). Heating at temperatures higher than 200°C produces two mass losses for all films. First occurring around 100°C attributed to the loss of physically adsorbed water molecules on the surface and zeolitic water and water trapped by egg-box model of Ca-crosslinked gel structure (Figure 6), and the second one, the decomposition of polymer between 200 and 250°C is attributed to the loss of half of the coordinated water in the bentonite layers and also to a partial decomposition of the biopolymer. It was suggested that[12] the biopolymer-LDH intercalation materials based on alginate show decomposition temperatures of the organic matter at almost the same temperature. This behavior called as protected effect consisted of increasing the thermal stability. Moreover, the exothermic peak at 200°C (around 12%) is related to the decomposition of chains, fragments, and monomers of alginate chains.[14] Increasing the weight loss at heating temperatures for higher than 280–400°C is related to combustion of the intercalated biopolymer and clays. Sharp peaks observed in pure alginate (1), and 1 : 1 of bentonite/alginate (2) at around 210 and 215°C could be related to the excess alginate that is not tightly bound to the bentonite substrate.[38] Increasing the bentonite concentration up to the region of the nonintercalated and agglomerated alginate film, exothermic

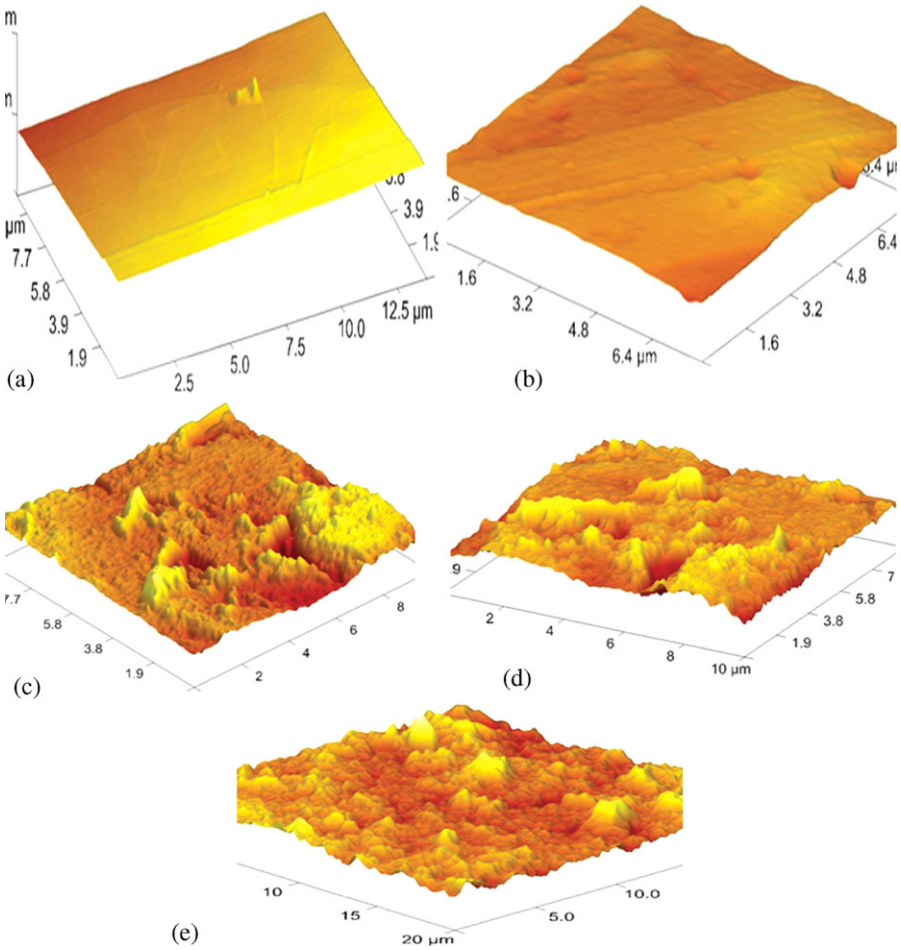

Figure 10. AFM images of the surfaces of pure alginate films (1 and 3 wt % of alginate, a and b), bentonite-added alginate film (c) and borax-bentonite-added alginate biocomposite films (d), respectively. [Color figure can be viewed in the online issue, which is available at wileyonlinelibrary.com.]

peak was also seen around 245°C which confirms higher dehydration of the bentonite (4). In contrast, the process at 240°C for borax addition and 215 and 320°C for (2) may be attributed to the decomposition of adsorbed alginate (without excess of alginate). This case is similar to the above results for the exfoliated structure with FTIR and XRD analyses for borax and smaller amount of bentonite addition, respectively. In this case, the higher thermal stability of borax-added bentonite/alginate biocomposite film could be attributed to the enhanced thermal stability of the native polymer. The influence of borate ions to the formation of complex gelling structure were provided together with borate ions[21] and egg-box model (Figure 6).

DMA

The temperature dependence of mechanical damping, tan δ, were obtained from the dynamic mechanical spectra's of composite films such as pure alginate and various bentonite-added alginate biocomposites (Figure 9). The enhancement and shift of tan δ peak to a higher temperature was obtained after the addition of smaller amounts of bentonite. The remarkable interactions and nanoreinforcement between alginate and hydroxyapatite nanocomposite hydrogels,[24] the effect of crosslinking by gluturaldehyde on the Na-alginate membrane,[41] and the comparison of uncrosslinked to crosslinked PVA/HPA nanocomposite membrane and intermolecular hydrogen bonding interactions between PVA chains and HPA particles[42] were also confirmed in literature. It is to be noted that this is basically in good agreement with our previous characterization analyses corresponding to the totally exfoliated structure below 3 wt %. However, the high bentonite caused the modulus to decrease. Increasing the bentonite concentration to the weight ratio of 1 : 12 as bentonite in alginate, tan δ value changed drastically from 0.37 to 0.18. Large agglomerates due to heterogeneous distribution of the filler also caused this behavior, but the shift in tan δ peak can be given as an indication of higher thermal degradation representing "clay effect" as expected in polymer-filler composite systems.[8,43] Moreover, the height of the tan δ peak gives information on the flexibility of the polymer. Increasing the filler content in the alginate films make them more rigid and loses their elasticity and flexibility are lost due to the height of the tan δ peaks. It can be easily deduced that significant improvement on the flexibility of alginate biocomposite was obtained with the addition of borax. For the same bentonite content, the addition of borax into the alginate enhanced the flexibility (the height of the tan δ peaks) from 0.2590 to 0.3200, respectively.

AFM Morphology

AFM images were used to characterize the morphologies of alginate biocomposite films specified for the surfaces of pure alginate (1 and 3 wt %), bentonite-added alginate, and borax-bentonite-added alginate biocomposite films, respectively (Figure 10). In all the images, the lighter part is the filler and the darker part is the polymer. Also, individual particles were determined on the nanocomposite surface utilizing the Phase AFM image in noncontact mode at 10 μm^2 scanning area. Encapsulated bentonite [Figure 10(c)] and, the intercalation of bentonite were directly confirmed at smaller bentonite content in alginate films. Moreover, the ionization of carboxylic acid groups, and the borate ions to produce -didiol complexes[21] also increased the interactions with hydrogen bonds and in turn the dispersions of fillers in the matrix [Figure 10(e)].

CONCLUSIONS

The results of this study can be summarized as follows;

1. Hydrocyclone purification of bentonite and several recrystallization steps for borax, are important to obtain more compatibile filler with hybrid properties
2. The casting and solvent evaporation technique can be conveniently used in the preparation of hybrid borax and bentonite-added alginate biocomposites.
3. Gelling processes were proved not only by Ca ions crosslinking known as egg-box model but also synergistic effect of borate ions as a crosslinking agent on the junction zones as borate-alginate complexes.
4. The physical properties of biocomposites can be changed by adjusting the level of bentonite concentration in the biocomposite.
5. The addition of bentonite to the alginate biocomposite caused new hydrogen bonding sites. Moreover, borax provided higher thermal stability to the bentonite/alginate biocomposite film. This could be attributed to the monodiol-borate complex formation between borate ions and hydroxyl groups of alginate sugar units as well as the cross-linking formation between didiol-borate complexes.
6. Borax as second inorganic filler is expected to have potential applications in the biocomposite area where environmentally friendly materials are preferred for enhanced compatible and flexible polymer films as well as improved structural and thermal properties.

REFERENCES

1. Zee, M. Handbook of Biodegradable Polymers, Bastioli, C., Ed.; Rapra Technology Limited: UK, **2005**.
2. Rhima, J. W.; Perry, K.; Ng, W. *Crit. Rev. Food Sci. Nutr.* **2007**, *47*, 411.
3. Flieger, M.; Kantorova, M.; Prell, A.; Rezanka, T.; Votruba, J. *Folia Microbiol.* **2003**, *48*, 27.
4. Yang, K.; Wang, X. L.; Wang, Z. *J. Ind. Eng. Chem.* **2007**, *13*, 485.
5. Wang, S. F.; Shena, L.; Tong, Y. J.; Chen, L.; Phang, I. Y.; Lim, P. Q.; Liu, T. X. *Polym. Degrad. Stab.* **2005**, *90*, 123.
6. Chivrac, F.; Pollet, E.; Schmutz, M.; Avérous, L. *Carbohyd. Polym.* **2010**, *80*, 145.
7. McGlashan, S. A.; Halley, P. *J. Polym. Int.* **2003**, *52*, 1767.
8. Alexandre, M.; Dubois, F. *Mater. Sci. Eng.* **2000**, *28*, 1.
9. Bordes, P.; Pollet, E.; Averous, F. *Prog. Polym. Sci.* **2009**, *34*, 125.
10. Hussain, F.; Hojjati, M.; Okamoto, M.; Gorga, R. E. *J. Compos. Mater.* **2006**, *40*, 1511.
11. Yang, L.; Liang, G.; Zhang, Z.; He, S.; Wang, J. *J. Appl. Polym. Sci.* **2009**, *114*, 1235.

12. Darder, M.; Lopez-Blanco, M.; Aranda, P.; Leroux, F.; Ruiz-Hitzky, E. *Chem. Mater.* **2005**, 17, 1969.
13. Ray, S. S.; Bousmina, M. *Prog. Mater. Sci* **2005**, *50*, 962.
14. Parhi, P.; Ramanan, A.; Ray, A. R. *J. Appl. Polym. Sci.* **2006**, *102*, 5162.
15. Smidsrod, O.; Draget, K. I. *Carbohydr. Eur.* **1996**, *14*, 6.
16. Grant, G. T.; Morris, E. R.; Rees, D. A.; Smith, P. J. C.; Thom, D. *FEBS Lett.* **1973**, *32*, 195.
17. Ma, P. X.; Elisseeff, J. H. In Scaffolding in Tissue Engineering. CRC Press, Taylor and Francis Group: Boca Raton, FL, **2006**.
18. Ruiz-Hitzky, E.; Darder, M.; Aranda, P. An introduction to bio-nanohybrid materials. In Bio-Inorganic Hybrid Nanomaterials, Ruiz-Hitzky, E.; Ariga, K.; Lvov, L. M., Eds.; Wiley: Weinheim, **2008**.
19. Rhim, J. W.; Ng, P. K. W. *Crit. Rev. Food Sci. Nutr.* **2007**, *47*, 411.
20. Coviello, T.; Coluzzi, G.; Palleschi, A.; Grassi, M.; Santucci, M.; Alhaique, F. *Int. J. Biol. Macromol.* **2003**, *23*, 83.
21. Pezron, E.; Ricard, A.; Lafuma, F.; Audebert, R. *Macromolecules* **1988**, *21*, 1121.
22. Gao, S.; Guo, J.; Nishinari, K. *Carbohydr. Polym.* **2008**, *72*, 315.
23. Benli, B.; Assemi, S.; Nalaskowski, J.; Çelik, M. S.; Miller, J. D. *J. Adhes. Sci. Technol.* **2011**, *25*, 1159.
24. Bouropoulos, N.; Stampolakis, A.; Mouzakis, D. E. *Sci. Adv. Mater.* **2010**, *2*, 239.
25. Coradin, T.; Nassif, N.; Livage, J. *Appl. Microbiol. Biotechnol.* **2003**, *61*, 429.
26. Bain, J. A.; Morgan, D. *J. Clay Miner.* **1982**, *18*, 33.
27. Bloodworth, A. J.; Morgan, D. J.; Briggs, D. A. *Clay Miner.* **1989**, *24*, 539.
28. Mullin, J. W. Crystallization, 3rd ed.; Butterworth-Heinemann Ltd.: Oxford, **1993**.
29. Li, L.; Fang, Y.; Vreeker, R.; Appelqvist, I. *Biomacromolecules* **2007**, *8*, 464.
30. Benli, B.; Boylu, F.; Karakaş, F.; Can, M. F.; Çinku, K.; Ersever, G. *J. Appl. Polym. Sci.* **2011**, *122*, 19.
31. Park, H.; Hong, J. H.; Ahn, K. H.; Lee, S. H.; Lee, J. *Korea-Aust. Rheol. J.* **2005**, *17*, 79.
32. Balaskrishnan, B.; Jayakrishnan, A. *Biomaterials* **2005**, *26*, 3941.
33. Xiao, C.; Lu, Y.; Liu, H.; Zhang, L. *Pure Appl. Chem.* **2000**, *37*, 1663.
34. Drelich, J.; Miller, J. D. *Miner. Metall. Process* **1995**, *12*, 197.
35. Sartori, C.; Finch, S. D.; Ralph, B. *Polymer* **1997**, *38*, 43.
36. Nayak, P. S.; Singh, B. K. *Bull. Mater. Sci.* **2007**, *30*, 235.
37. Gunister, E.; Pestreli, D.; Unlu, C. H.; Atici, O.; Gungor, N. *Carbohydr. Polym.* **2007**, *67*, 358.
38. Darder, M.; Lopez-Blanco, M.; Aranda, P.; Aznar, A. J.; Bravo, J.; Ruiz-Hitzky, E. *Chem. Mater.* **2006**, *18*, 1602.
39. Caykara, T.; Demirci, S.; Eroglu, M. S.; Guven, O. *Polymer* **2005**, *46*, 10750.
40. Fischer, H. *Mater. Sci. Eng. C* **2003**, *23*, 763.
41. Ravindra, S.; Veerapur, K. B.; Gudasi, M.; Sairam, R. V.; Shenoy, M.; Netaji, K. V.; Raju, S.; Sreedhar, N.; Tejraj, B.; Aminabhavi, M. *J. Mater. Sci.* **2007**, *42*, 4406.
42. Teli, S. B.; Gokavi, G. S.; Sairam, S.; Aminabhavi, T. M. *Sep. Purif. Technol.* **2007**, *54*, 178.
43. Ray, S. S.; Okamoto, M. Polymer/layered silicate nanocomposites: a review from preparation to processing. *Prog. Polym. Sci.* **2003**, *28*, 1539.